Mechanism of Thermal Decomposition of Tetrabromobisphenol A (TBBA)

ARTICLE *in* THE JOURNAL OF PHYSICAL CHEMISTRY A · SEPTEMBER 2014

Impact Factor: 2.69 · DOI: 10.1021/jp505742u · Source: PubMed

2 AUTHORS:

Mohammednoor Altarawneh
Murdoch University
83 PUBLICATIONS **525** CITATIONS
SEE PROFILE

Bogdan Z Dlugogorski
Murdoch University
296 PUBLICATIONS **2,489** CITATIONS
SEE PROFILE

THE JOURNAL OF PHYSICAL CHEMISTRY A

Article

pubs.acs.org/JPCA

Mechanism of Thermal Decomposition of Tetrabromobisphenol A (TBBA)

Mohammednoor Altarawneh*,† and Bogdan Z. Dlugogorski

School of Engineering and Information Technology, Murdoch University, Perth 6150, Australia

Supporting Information

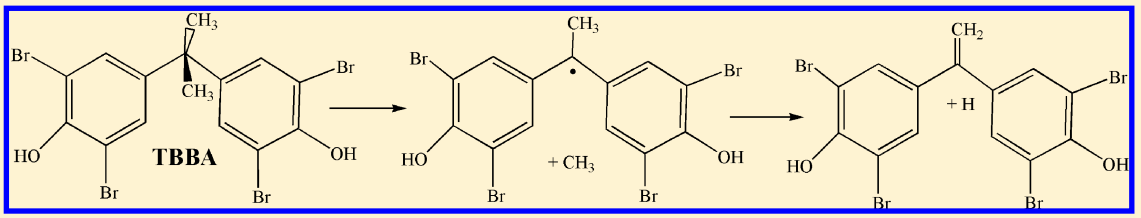

ABSTRACT: This study presents a detailed investigation into the gas-phase thermal decomposition of tetrabromobisphenol A (TBBA), that is, the most widely used brominated flame retardant (BFR). Elimination of one of the methyl groups characterizes the sole dominant channel in the self-decomposition of the TBBA molecule at all temperatures. A high-pressure rate constant for this reaction is fitted to $k(T) = 2.09 \times 10^{10} T^{1.93} \exp(-37000/T)$ s^{-1}. The high A factor and low activation energy for this reaction arise from the formation of a delocalized radical upon the loss of a methyl group. We calculate rate constants for the bimolecular reactions of TBBA with H, Br, and CH_3 radicals. Kinetic and mechanistic data provided herein should be instrumental to gain further understanding of the fate of TBBA during thermal degradation of materials laden with this BFR.

1. INTRODUCTION

Owing to their significant potentials to reduce the flammability tendency of polymeric materials, brominated flame retardants (BFRs) have been widely deployed during the last few decades in numerous consumers products.[1] Tetrabromobisphenol A (TBBA) currently constitutes nearly 60% of the world's total production and usage of BFRs. TBBA is also deployed as a reactant for the formation of other commercial BFRs. Bromine radicals formed during the degradation of TBBA delay ignition of overheated electronic and electrical devices.[2] As thermal treatment represents a mainstream strategy for disposal of materials laden with TBBA, the pyrolytic decomposition of TBBA has attracted mounting scientific attention.[3]

Several experimental studies have been carried out to address the decomposition of either pure TBBA or TBBA immersed in polymeric matrixes, under pyrolytic or oxidative conditions, typically in the range of 300−600 °C.[4−11] Major products from the pyrolysis of TBBA include HBr, brominated phenols, and benzenes, in addition to char and a wide range of brominated aromatics. Almost half of the initial bromine in the parent TBBA was found to transform into HBr.[9] The main environmental burden of using TBBA stems from the fact that its decomposition products, such as brominated phenols, serve as building blocks for the formation of polybrominated dibenzo-*p*-dioxins and polybrominated dibenzofurans (PBDD/Fs). Recent experimental studies on the pyrolysis of polymers containing TBBA have reported the formation of several congeners of PBDD/Fs.[8,12−14]

Suggested mechanisms for decomposition of TBBA involve loss of HBr, successive C−Br bond fission, cleavage of the isopropylidene linkage, a cross-linking condensation reaction, and bimolecular reactions involving radicals and TBBA.[9] Several kinetic models were constructed to account for the overall decay of TBBA and the formation of the experimentally observed products.[15] It was proposed that debromination and scission reactions, yielding brominated phenols, dominate the overall decomposition of TBBA. Marongiu et al.[9] validated their semidetailed kinetic model against several sets of experimental data. More recently, Font et al.[6] simplified the model of Marongiu et al.[9] and presented an abridged kinetic mechanism taking into account the nature of TBBA as a backbone BFR (as BFRs form part of the polymeric material itself). Thermochemical and kinetic data of this model were frequently carried over from those of analogous species and corresponding reactions. For instance, Marongiu et al.[9] derived rate constants for the prominent reactions in their comprehensive kinetic model from the analogous gas-phase reactions.

While the decomposition of TBBA mainly occurs in the condensed phase, gas-phase reactions contribute significantly to the overall decomposition of TBBA. Guided by their results on the volatility of TBBA, Marsanich et al.[16] explained that exposing TBBA to a temperature higher than its melting point (~450 K) results readily in the evaporation of TBBA. Barontini et al.[15] showed that the evaporation of TBBA contributed significantly to the total weight loss of TBBA at temperatures as low as 480 K. Available kinetic models were primarily formulated to describe decomposition in the condensed phase. Thus, they are not extendable to account for the

Received: June 10, 2014
Revised: September 4, 2014
Published: September 18, 2014

dx.doi.org/10.1021/jp505742u | J. Phys. Chem. A 2014, 118, 9338−9346

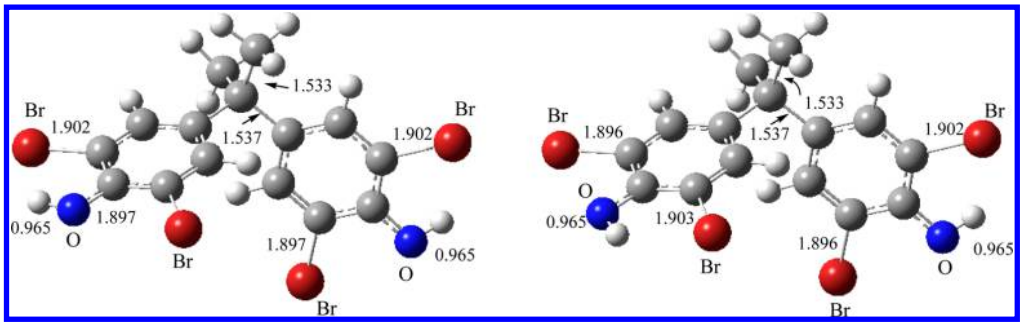

Figure 1. Optimized structures of the TBBA molecule. Interatomic distances are in Å.

Scheme 1

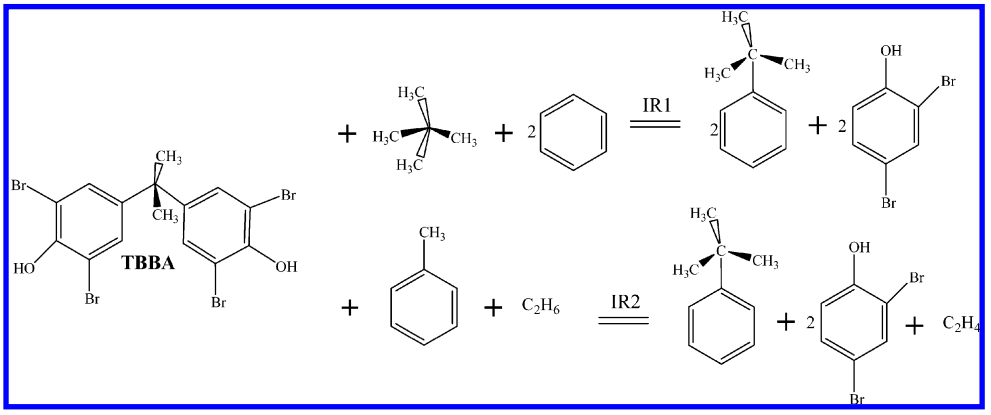

decomposition chemistry of TBBA in the gas phase. A kinetic gas-phase model of the pyrolysis of TBBA differs fundamentally from a corresponding condensed-phase model. For example, bimolecular isomerization reactions (prevailing reactions in the condensed phase) are of negligible importance when compared with the unimolecularly derived pathways in the gas phase. Furthermore, understanding the gas-phase decomposition of TBBA will shed more light on the complex kinetic phenomena occurring in the condensed medium.

To this end, this study presents a detailed theoretical account of mechanisms governing the gas-phase decomposition of TBBA. The objective is to analyze, on a precise molecular basis, all pathways operating during the self-decomposition of TBBA and its bimolecular reactions with prominent radicals in the pyrolytic medium. This study follows our earlier investigations on decomposition of prominnet BFRs[17] and represents another contribution to gain further understanding into the environmental impact of application of BFRs for improved fire safety of polymeric materials.

2. COMPUTATIONAL DETAILS

We have deployed the Gaussian 09[18] program to perform all structural optimizations at the M062X/6-311+G(d,p) level of theory. M062X[19] constitutes a new hybrid meta exchange correlation functional. It has been parametrized against large databases of experimental and highly accurate, theoretically derived values, to yield very precise thermochemical and kinetic properties. As energies from M05-M06 DFT functionals are generally sensitive to the deployed quadrature grid, we have used an integration grid that spans 99 and 590 radial and angular points, correspondingly. We have shown recently[17] that deploying a higher grid density (120 radial and 590 angular points) changes the calculated reaction energies by only 0.02−0.05 kcal/mol. In order to increase the accuracy of our calculated reaction and activation enthalpies, single-point energy calculations were carried out at the extended basis set of GTLarge.[20] Applying a bigger basis set has changed final energies only marginally, within 1.0 kcal/mol, in reference to the corresponding results obtained with the 6-311+G(d,p) basis set. Intrinsic reaction coordinates (IRCs) confirm the nature of each transition structure by connecting it to its corresponding reactants and products.

The Supporting Information comprises Cartesian coordinates, energies, and vibrational frequencies for all structures. We obtained the reaction rate constants in the high-pressure limit by applying the conventional transition state theory (TST). Transmission factors based on Wigner's formula[21] provided corrections to the reaction rate constants owing to the tunnelling effects. The plausible degenerate numbers of reactions sites and the C_2 symmetry of the TBBA were accounted for in the calculated reaction constants. In the computations, weak structural buckling motions were treated as harmonic oscillators because their effects cancel out due to their existence both in the reactants and the transition states. These buklings correspond to small values of vibrational frequencies (<10 cm^{-1}), involving mainly the C−$(CH_3)_2$−C bridge. A pressure-dependent reaction rate constant was calculated for one reaction using the RRKM theory.[22] We adopted the Lennard-Jones parameters for the TBBA molecule from analogous values of the diphenyl ether molecule. Kinetic calculations were carried out with the aid of the ChemRate code.[23] On the basis of the adapted methodology, we anticipate maximum uncertainty limits in the calculated activation energy (E_a) to be within ±1−3.0 kcal/mol, that is, the accuracy margin of the adapted methodology.[19]

dx.doi.org/10.1021/jp505742u | J. Phys. Chem. A 2014, 118, 9338−9346

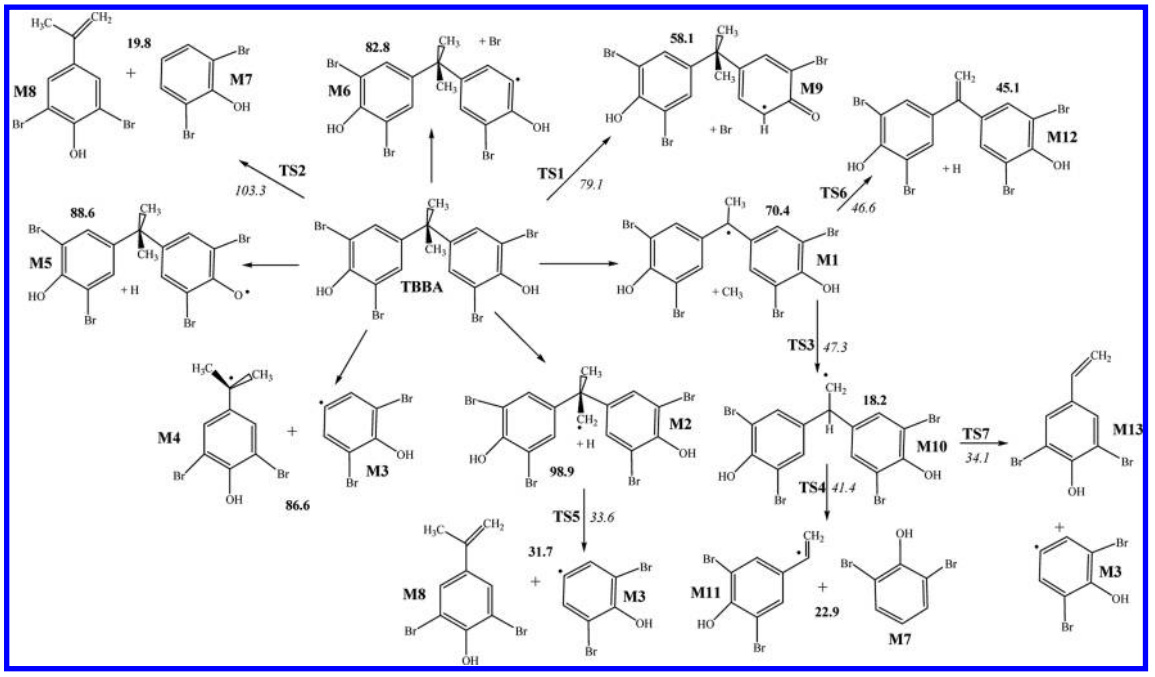

Figure 2. PES for the self-decomposition of the TBBA molecule. Values in bold and italics signify reaction and activation energies at 0.0 K. Five of the seven initial exit channels are barrierless.

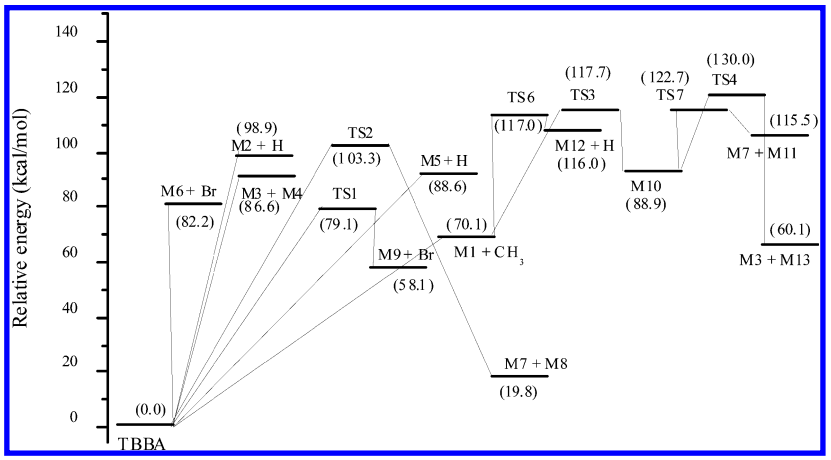

Figure 3. Relative PES for the self-decomposition of the TBBA molecule. All values are at 0.0 K.

3. RESULTS AND DISCUSSION

3.1. Structure and Thermochemistry of TBBA. Figure 1 depicts the optimized structures of the TBBA molecule. Depending on the orientation of the OH group in the TBBA molecule, the molecule exhibits several conformers. Figure 1 portrays two of these conformers. The C−Br bond lengths in both conformers seem to be slightly affected by the orientation of the OH group and differ by ∼0.083 Å. Nevertheless, the energy gap between the two conformers is calculated to be 0.06 kcal/mol, the quantity that most likely falls within the accuracy margin of the adapted theoretical methodology. Our calculated geometries at the M062X/6-311+G(d,p) level of theory agree very well with the corresponding experimental measurements[24] and recent theoretical predictions at the B3LYP/6-31G(d) level of theory.[25] For instance, the computed C−CH_3 and C−Br bond lengths amount to 1.533 and 1.903/1.896 Å, that is, they remain in excellent agreement with the corresponding experimental values of 1.533 and 1.877 Å, respectively. Overall, TBBA displays, to a great extent, geometrical features similar to those of bromophenols.

To the best of our knowledge, the literature reports no standard enthalpy of formation of gaseous TBBA. For this reason, we calculate $\Delta_f H^\circ_{298}$ of the TBBA molecule using the isodesmic reactions in Scheme 1.

These reactions rely on the accurate experimental values of $\Delta_f H^\circ_{298}$ for reference species,[26] yielding $\Delta_f H^\circ_{298}$ of −38.5 and −39.3 kcal/mol for isodesmic reactions IR1 and IR2, respectively. It follows that,an average value of $\Delta_f H^\circ_{298}$ for the TBBA molecule can be assigned a value of −38.9 kcal/mol with an uncertainty of ±0.6 kcal/mol, that is, one standard deviation associated with the two calculated $\Delta_f H^\circ_{298}$ values of IR1 and IR2 reactions. We recommend using this value in kinetic modeling until an experimental determination becomes available. Finally, we remark that the experimental $\Delta_f H^\circ_{298}$ exists only for the 2,4-dibromophenol, forcing us to perform the calculations based on this congener. Nonetheless, we expect close results for 2,6-dibromophenol, should its $\Delta_f H^\circ_{298}$ be available.

dx.doi.org/10.1021/jp505742u | J. Phys. Chem. A 2014, 118, 9338−9346

3.2. Initial Decomposition of TBBA. Figure 2 illustrates the detailed potential energy surface (PES) for the initial decomposition of the TBBA molecule, with Figure 3 depicting corresponding relative energies in reference to the parent TBBA molecule. The decomposition of TBBA branches into seven initial exit channels. Fission of one of the C−CH_3's requires the lowest energy change of reaction among all initial channels. This barrierless reaction is associated with an endoergicity of 70.4 kcal/mol and produces the double resonantly stabilized benzilic-type radical of M1. Cleavage of the isopropylidene linkage in TBBA and the subsequent formation of the two radicals, M3 and M4, incur an endoergicity of 86.6 kcal/mol. Fission of the O−H bond and generation of the phenoxy-type radical of the M5 moiety necessitates a considerable energy of 88.6 kcal/mol. This value concurs with that reported in the literature of 87.2 kcal/mol for the bond dissociation enthalpy (BDE) of O−H in 2-bromophenol.[27] Rupture of the aromatic C−Br bond requires an endoergicity of 82.8 kcal/mol. Considering the experimental BDE of C−Br in bromobenzene of 83.5 kcal/mol,[27] we deduced that the presence of the neighboring hydroxyl group induces no effect on the strength of the C−Br bond in the TBBA molecule. Our calculated BDE for H_2C−H, leading to the formation of the M2 moiety (98.9 kcal/mol), agrees with the corresponding BDE in neopentane of 99.4−100.3 kcal/mol.[27] The agreement between our calculated BDE estimates and the analogous literature values confirms the accuracy of the M062X theoretical approach in deriving thermochemistry pertinent to the self-decomposition of the TBBA molecule.

In addition to the five barrierless bond fissions, intramolecular hydrogen transfers via the transition structures TS1 and TS2 open two plausible exit channels. Hydrogen migration from the hydroxyl group to *ortho*-carbon atoms releases a bromine atom and results in the formation of the phenoxy-type radical of M9. The transition state of this reaction (TS1) resides 79.1 kcal/mol above the initial reactant. This barrier is significantly lower than the activation energy required for the corresponding phenolic H transfer (91.4 kcal/mol) into an *ortho*-C(Cl) site in the 2-chlorophenol molecule.[28] This noticeable difference could be rationalized in view of a weaker aromatic C−Br bond in comparison to the aromatic C−Cl bond, that is, 83.3 versus 95.5 kcal/mol. The release of bromine atoms through this reaction is accompanied by an endoergicity of 58.8 kcal/mol. In the other intramolecular hydrogen-transfer reaction, a 2,6-dibromophenol (M7) and 2,6-dibromo-4-(prop-1-en-2-yl)phenol (M8) molecules form upon hydrogen migration from one of the methyl groups to the *para*-carbon on the aromatic ring. However, the exceedingly high activation energy (103.3 kcal/mol) makes this reaction unlikely to proceed in practical systems.

As the formation of the M1 moiety is associated with the lowest energetic requirements in the initial decomposition of the TBBA molecule, we address its self-decomposition further. There are two competing exit channels for the M1 radical, direct β C−H bond fission in the methyl group and intermolecular H transfer. Direct fission of one of the β C−H bonds in the methyl group requires an activation energy of 46.6 kcal/mol (TS6), slightly higher than the calculated reaction energy (45.1 kcal/mol) of this process. This channel produces the 4,4′-(ethene-1,1-diyl)bis(2,6-dibromophenol) moiety (M12). Alternatively, the M10 radical arises by a hydrogen atom shift from the methyl group onto the radical site of the bridge carbon, through a sizable activation energy of 47.3 kcal/mol (TS3). M10 branches into two pathways. Direct β C−C bond fission via TS7 (34.1 kcal/mol) requires lower activation energy than the intermolecular hydrogen transfer through TS4 (41.4 kcal/mol). The former channel produces the dibromophenol phenyl-type radical (M3) and the 2,6-dibromo-4-vinylphenol molecule (M13). A second hydrogen migration step from the H(C)CH_2 bridge in M10 and subsequent splitting of the C−C bridge afford the 2,6-dibromophenol molecule (M7) and the M11 radical. An analogous β C−C bond fission in the M2 intermediate leads to the 2,6-dibromophenol phenyl-type radical (M3) and the M8 molecule via a modest energy barrier of 33.6 kcal/mol.

On the basis of reaction and activation energies given in Figure 2, we envisage that two channels most likely dominate the initial decomposition of the TBBA molecule, namely, barrierless fission of the methyl group and the intramolecular phenolic hydrogen transfer via TS1. In order to assess their relative importance, we calculate the reactions rate constants in the high-pressure limit for these two channels and fit them to modified Arrhenius expressions in the temperature range of 400−1500 K. Deriving a rate constant for the barrierless reaction (TBBA → M1 + CH_3) necessitates treatment within the framework of the variational transition state theory (VTST). The VTST minimizes the calculated reaction constant as a function in temperatures and reaction coordinates.[29] The implementation procedure of VTST is described in detail elsewhere. To deploy the VTST on the (TBBA → M1 + CH_3) requires constructing a minimum-energy point (MEP) curve along the stretching of the C−CH_3 bond. As DFT functionals are single-reference character methods, they suffer from a fundamental shortcoming in describing singlet−triplet crossing involved in the C−CH_3 bond breakage. However, implementation of a multireference character method such as CASSAF or CASPT2 on a system as large as the TBBA molecule is prohibitively expensive computationally.[30] Furthermore, the TBBA molecule contains a very large number of electron configurations that in turn makes it a daunting task to select appropriate active spaces and electrons. Alternatively, the pioneering work of Yamagushi's group,[31,32] over the last two decades, has demonstrated that energies of biradical systems calculated by any single-determinant method can be significantly improved via the application of a simple approximated spin-projection scheme (AP). In this scheme, an approximated spin-projected energy (E^{AP}) can be derived from energies of broken-symmetry (E^{BS}) and pure high-spin (E^{HS}) states as

$$E^{AP} = f^{AP}E^{BS} - (f-1)E^{HS}$$

where f^{AP} denotes the spin-projection factor

$$f^{AP} = \frac{\langle S^2\rangle^{HS} - s(s+1)}{\langle S^2\rangle^{HS} - \langle S^2\rangle^{BS}}$$

with $\langle S^2\rangle^{HS}$ and $\langle S^2\rangle^{BS}$ signifying expectation values of spin contamination pertinent to pure high-spin and broken-symmetry states, respectively. It was found that the application of the AP approach to various biradical systems yielded DFT-derived energies within 1.0−3.0 kcal/mol of corresponding values obtained with the more expensive multireference methods. Figure 4 portrays our MEP curve for the C−CH_3 bond fission based on the AP formalism. Candidates of transition structures for the barrierless fission of the C−CH_3 are located at C···CH_3 separations of 2.7−2.8 Å. In these structures, rotation around the C−CH_3 bond in the parent

dx.doi.org/10.1021/jp505742u | J. Phys. Chem. A 2014, 118, 9338−9346

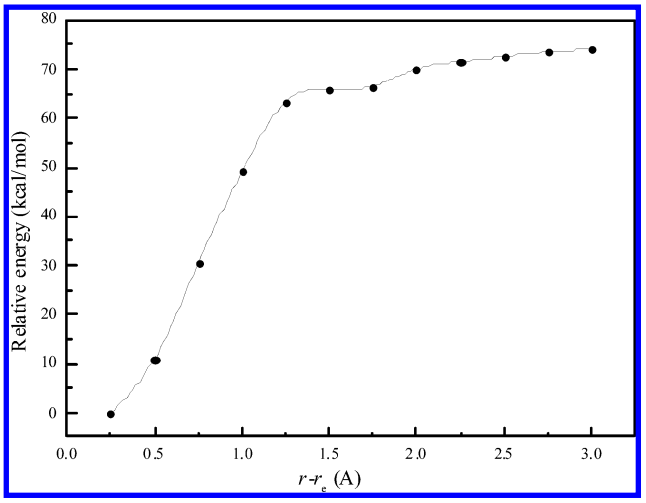

Figure 4. Energy profile for the barrierless reaction TBBA → M1 + CH_3. The relative zero-point corrected energy (0 K), plotted on the ordinate axis, refers to the energy with respect to the initial energy of the TBBA reactant.

TBBA molecule transforms into stretching vibration along the C−CH_3 fission reaction coordinate.

The TST allows calculation of the reaction rate constant for the reaction (TBBA → M9 + Br). Table 1 documents the fitted rate constant parameters. Clearly, fission of the C−CH_3 bond constitutes the sole important channel in the gas-phase initial decomposition of the TBBA molecule at all temperatures. Our finding here differs somewhat from the behavior of the self-decomposition of the 2-chlorophenol system,[28] in which the transfer of phenolic H holds more importance than all other available channels. The significance of the C−CH_3 bond cleavage as the most favored initiator pathway was also highlighted by Marongiu et al.[9]

In order to provide a benchmark for the accuracy of our calculated rate constant for the fission of the C−CH_3 bond, Figure 5 compares our computed rate constant with the experimental values of the analogous decomposition reaction, C_6H_5−C(CH_3)$_2$−C_6H_5 → C_6H_5−C(CH_3)−C_6H_5 + CH_3, determined experimentally by Robaugh et al.,[33] $k(T(\mathrm{K})) = 5.01 \times 10^{15} \exp(-33000/T)$ s^{-1}, and the derived expression by Marongiu et al.,[9] $k(T(\mathrm{K})) = 3.0 \times 10^{13} \exp(-25300/T)$ s^{-1}. The three sets of data show reasonable agreement at elevated temperature (T > 1000 K). While our fitted activation energy (E_a) overshoots slightly the value of Robaugh et al.,[33] 74.0 versus 66.0 kcal/mol, our A factor falls within 1 order of magnitude with respect to the measurements of ref 28 for CH_3 loss from the 2,2′-diphenylpropane molecule. A plausible explanation for the noticeable deviation between our calculated and corresponding literature values in Figure 5 can be attributed to the fact that the latter were adapted from analogous systems, that is, they were not measured specifically for the TBBA system.

Sivaramakrishnan et al.[34] have recently reported a significantly lower A factor of 8.66×10^{12} s^{-1} for the corresponding CH_3 release from neopentane at temperatures of 1260−1462 K and pressures of 0.2−1.0 atm. In order to compare our calculated rate constant for fission of the C−CH_3 bond under similar conditions, we have utilized the RRKM theory to derive the rate constants at a pressure of 0.75 atm and a temperature range of 400−1500 K. We fitted the title reaction to a rate expression of $k(T,0.75\ \mathrm{atm}) = 1.45 \times 10^{15} \exp(-36400/T)$ s^{-1}). A higher A factor in the case of the TBBA molecule, in reference to that of neopentane, could be rationalized by the

Table 1. Fitted Modified Arrhenius Parameters at the High-Pressure Limit[a]

reaction	A (s^{-1} or cm^3 $molecule^{-1}$ s^{-1})	n	E_a/R (K)
TBBA → M1 + CH_3	2.09×10^{10}	1.93	37000
TBBA → M9 + Br	3.16×10^{12}	0.44	40000
M1 → M10	1.62×10^{11}	0.66	23900
M1→ M12 + H	1.91×10^{10}	1.18	23500
M10 → M3 + M15	1.68×10^{11}	0.27	17500
M10 → M11 + M7	2.04×10^{10}	0.72	20800
TBBA + H → M5 + H_2	2.89×10^{-10}	0.00	6700
TBBA + H → M2 + H_2	2.52×10^{-9}	0.00	6900
TBBA + H → M17 + HBr	3.17×10^{-10}	0.00	5200
TBBA + H → M1 + CH_4	7.96×10^{-10}	0.00	16600
TBBA + H → M6 + HBr	2.52×10^{-9}	0.00	5300
TBBA + H→ M14	1.05×10^{-10}	0.00	4700
TBBA + H → M15	4.80×10^{-10}	0.00	3100
TBBA + H→ M16	5.77×10^{-11}	0.00	4600
M15→ M1 + CH_4	4.90×10^{13}	0.00	18800
M15→ M3 + M24	1.58×10^{15}	0.36	27200
M15→ M16	2.24×10^{13}	0.00	24800
TBBA + Br → M5 + HBr	3.03×10^{-10}	0.00	3200
TBBA + Br → M2 + HBr	1.55×10^{-9}	0.00	7200
TBBA + CH_3 → M2 + CH_4	8.12×10^{-12}	0.00	8600
TBBA + CH_3 → M5 + CH_4	2.51×10^{-12}	0.00	6300
TBBA + CH_3 → M6 + CH_3Br	3.01×10^{-11}	0.00	10200
TBBA + CH_3 → M19 + Br	3.89×10^{-13}	0.00	6600
TBBA + CH_3 → M20	3.54×10^{-13}	0.00	7400
TBBA + CH_3 → M21	9.72×10^{-13}	0.00	7700
M5 → M4 + M22	2.88×10^{13}	0.54	27000
M5 → M8 + M23	2.88×10^{11}	0.82	30000

[a]In a temperature range of 400−1500 K. These parameters follow a modified Arrhenius rate expression, $k(T(\mathrm{K})) = AT^n \exp(-E_a/RT)$.

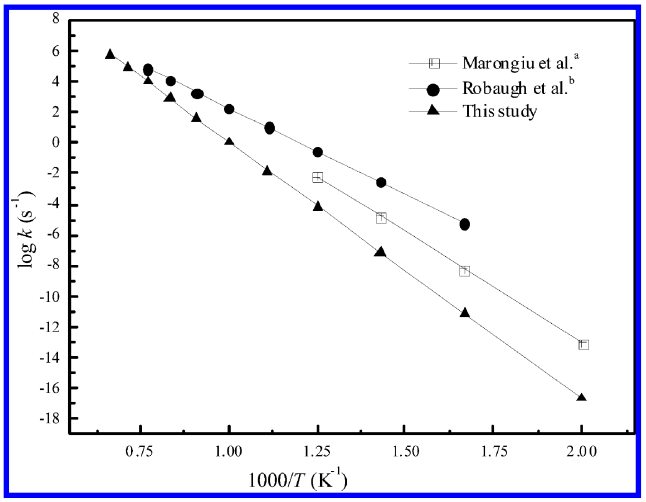

Figure 5. Arrhenius plots comparing the calculated and literatures values for the (TBBA → M1 + CH_3) reaction. [a]Reference 9; [b]reference 33.

dx.doi.org/10.1021/jp505742u | J. Phys. Chem. A 2014, 118, 9338−9346

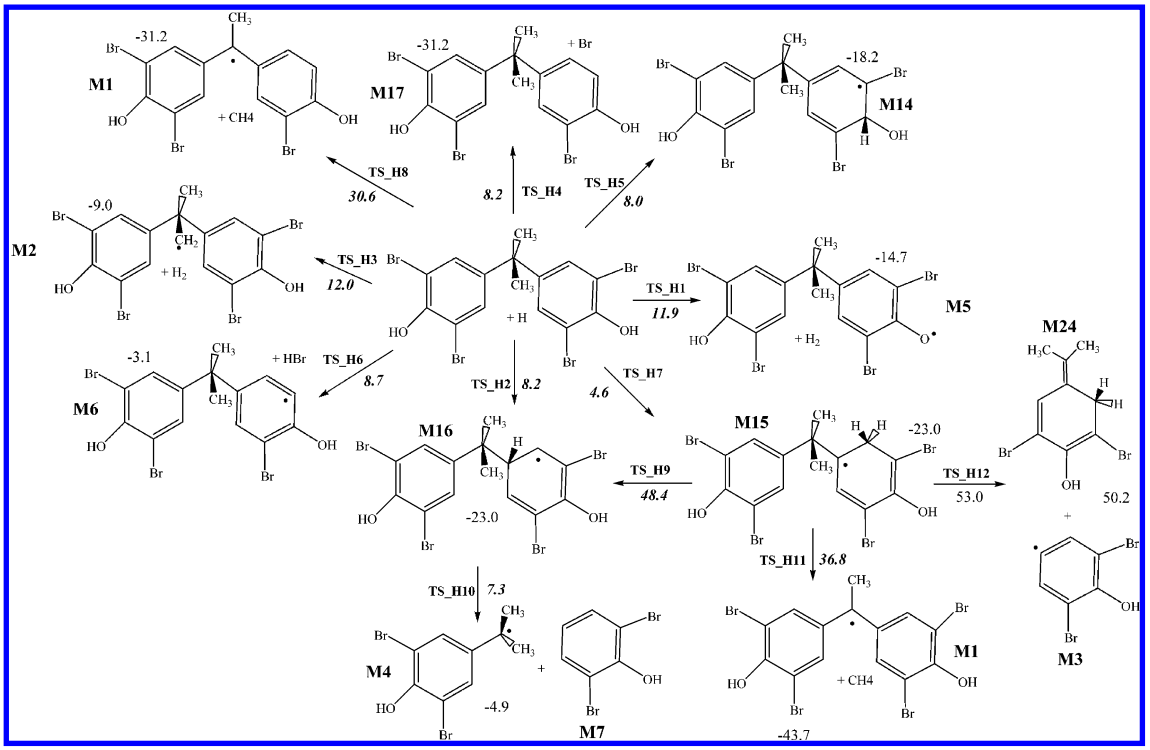

Figure 6. PES for the self-decomposition of TBBA in bimolecular reactions with H atoms. Values in bold and italics signify reaction and activation energies at 0.0 K.

conjugated π-electron networks in the delocalized radical of M1, which in turn acts to assist C−CH_3 bond fission in reference to the localized radical $C(CH_3)_3$ (neopentane). Figure S1 in the Supporting Information reports ratios of $k(T,\text{high-}P)/k(T,1\text{ atm})$. It is evident from Figure S1 (Supporting Information) that the C−CH_3 bond fission exhibits strong pressure-dependent behavior, especially at high temperatures. It is worthwhile mentioning that the seven pathways explored in Figure 2 exhibit fewer energy-demanding requirements than that of the fission of the aromatic C−H bond (BDH = 111.0 kcal/mol).

Calculated reaction rate constants for the two competing exit channels of M1 indicate a fraction of around 0.87 for the direct β C−H bond fission in the considered temperature range of 400−1500 K. The relative importance of intermolecular hydrogen transfer forming the M10 moiety remains virtually constant at 0.12−0.13. The entire PES presented in Figure 2 and calculated reaction rate constants conclude that the unimolecular decomposition preferentially generates the M12 (4,4′-(ethene-1,1-diyl)bis(2,6-dibromophenol) intermediate with small (but not negligible) product flux into M13 and M3.

The formation of the three major products (M12, M3, and M13) accompanies the generation of two important radicals, H and CH_3. Furthermore, TBBA forms miscible formulations with the treated polymeric materials. The latter serve as potent sources for hydrogen atoms. As explained by Marongiu et al.,[9] Br atoms arise through a series of complex heterogeneous reactions in the condensed phase during the thermal degradation of the TBBA molecule. It follows that the reactions of the TBBA molecule with H, Br, and CH_3 radicals exhibit crucial importance in practical pyrolysis processes. In the next sections, we present mechanisms and kinetic parameters for these reactions.

3.3. Reactions of TBBA with Hydrogen Atoms. Figure 6 illustrates eight distinct channels reactions of H atoms with the TBBA molecule. Addition at an aromatic C(H) site requires the lowest energy of activation of 4.6 kcal/mol via the transition structure TS_H7. The formed M15 moiety lies in a deep energy well of −23.0 kcal/mol, in reference to the separated reactants. Additions at C(OH), *ipso*-isopropylidene, and C(Br) sites incur very similar activation energies in the range of 8.0−8.2 kcal/mol, with the addition at the C(Br) involving the simultaneous Br departure via the transition structure TS_H4. Abstraction of phenolic and methyl H atoms demands virtually the same activation energy, that is, 11.9 and 12.0 kcal/mol, respectively. Abstraction of bromine atoms proceeds with a reaction energy of 8.7 kcal/mol (TS_H6). Abstraction of a methyl group via TS_H8 involves the highest activation energy (30.6 kcal/mol) among the initial TBBA + H channels.

Table 1 documents the fitted rate parameters for the seven plausible TBBA + H reactions. On the basis of these parameters, Figure 7 portrays the branching ratios for all channels. The addition at a C(H) site and Br abstraction constitute the two most important channels. Lower activation energy for the H-addition channel (M15) and higher entropy of activation for the Br-abstraction channel (M6 + HBr) lead to channel switching, observed as a function of temperature. The rate of hydrogen addition at the C(H) site exceeds the rate of bromine abstraction up to a temperature of 1300 K. The dominance of the Br-abstraction channel in the TBBA + H system contributes to the high yield of HBr detected from the pyrolysis of TBBA.

Three exit channels are available for the M15 intermediate, the 1,2-hydrogen shift reaction forming the M16 moiety, direct cleavage of the C−C bond, and elimination of a CH_4 molecule. Activation energies for these three channels are calculated as 48.4 (TS_H9), 36.8 (TS_H11), and 53.0 kcal/mol (TS_H12),

dx.doi.org/10.1021/jp505742u | J. Phys. Chem. A 2014, 118, 9338−9346

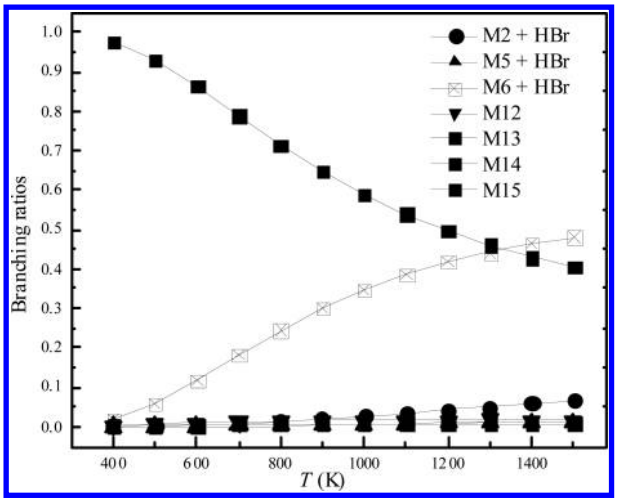

Figure 7. Branching ratios for TBBA + H reactions.

respectively. Examination of reaction rate constants in Table 1 reveals that the exclusion of a methane molecule is significantly more important than the intramolecular migration of hydrogen and the direct C−C bond cleavage.

3.4. Reactions of TBBA with Bromine Atoms. Figure 8 shows a schematic of plausible reactions of the TBBA molecule with a Br atom. These reactions were also suggested by Barontini et al.[15] in their mechanistic analysis of the TBBA pyrolysis. Scission of the isopropylidene linkage via bromine addition at an ipso site produces 2,4,6-tribromophenol molecule and the M4 radical. This reaction occurs through an energy barrier of 14.3 kcal/mol (TS_Br2). Hydrogen abstraction from the methyl moiety, hydroxyl group, and the aromatic ring requires activation energies of 11.8, 7.1, and 23.1 kcal/mol, respectively. The ordering of these barriers is in line with the corresponding bond dissociation energies of C−H and O−H. The kinetic parameters listed in Table 1 reveal the competitive nature of the H abstraction from methylic and hydroxyl groups at temperatures higher than 800 K and the lesser importance of the fission of the isopropylidene bridge at all temperatures. Our finding here differs from the interpretation of Barontini et al.[15] with regard to the potential formation of brominated phenols via Br-induced addition at the edge of the isopropylidene linkage. Despite our best attempts, we were unable to locate transition structures for addition of a Br atom to aromatic rings in the TBBA molecule. In fact, halogens react with aromatic compounds mainly via H-abstraction channels, even at low temperatures.[35,36]

3.5. Reactions of TBBA with the Methyl Group. As shown in Figure 9, reactions of the TBBA molecule with a methyl radical branch into six pathways. Abstraction of a hydroxyl H characterizes the most favorable pathway with a trivial activation energy of 8.9 kcal/mol and an exothermicity of 15.0 kcal/mol. Calculated reaction rate parameters for the six TBBA + CH_3 channels in Table 1 confirm the dominance of this pathway at all temperatures. Abstraction of methyl H atoms and additions to the aromatic ring are predicted to be of negligible importance at all temperatures.

The intermediate M5 represents a main product from bimolecular reactions of TBBA with Br and CH_3 radicals. The apparent fate of the phenoxy-type radical of M5 is to undergo a ring contraction/CO elimination mechanism to yield a five-membered ring structure in analogy to the well-established mechanism involving phenoxy radicals.[37] Detection of small amounts of CO/CO_2 during the pyrolysis of TBBA supports the occurrence of the ring contraction/CO elimination mechanism.

Additionally, the fate of the M5 moiety is controlled by two competing reactions, shown in Scheme 2.

Hydrogen transfer from the methyl group and subsequent fission of the C−C bridge via TS8 requires an activation energy of 59.8 kcal/mol. Alternatively, direct β C−C bond fission occurs through TS9. Activation energy associated with TS9 amounts to 53.2 kcal/mol. Products from TS8 and TS9 reside 26.6 and 50.1 kcal/mol above M5, respectively. Barriers of these two reactions are close to the overall barrier of the competitive contraction/CO elimination mechanism (58.0−

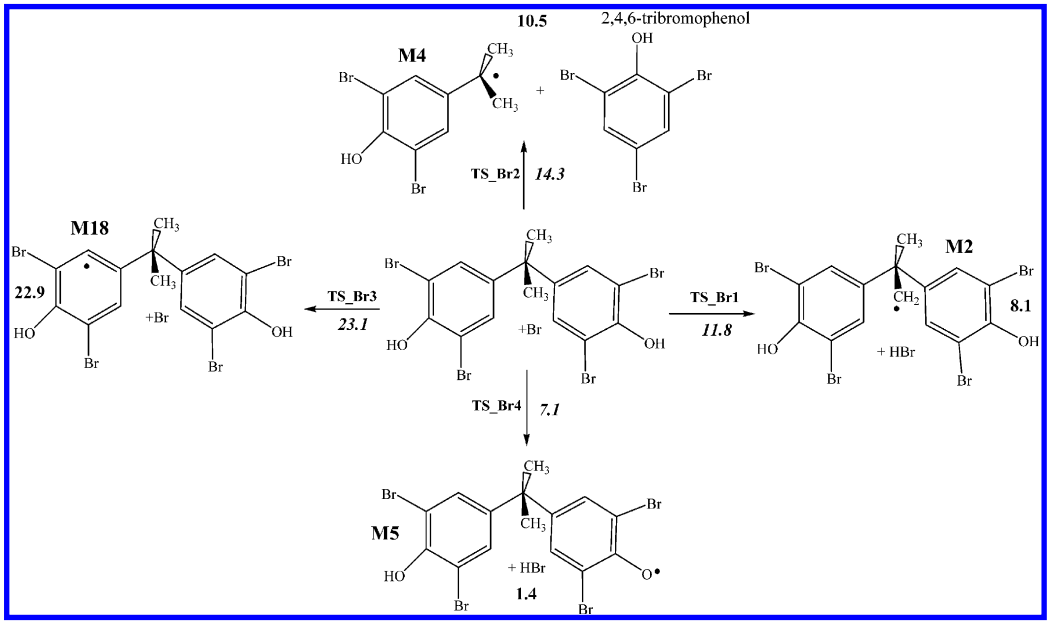

Figure 8. PES for the decomposition of TBBA in bimolecular reactions with Br atoms. Values in bold and italics signify reaction and activation energies at 0.0 K.

dx.doi.org/10.1021/jp505742u | J. Phys. Chem. A 2014, 118, 9338−9346

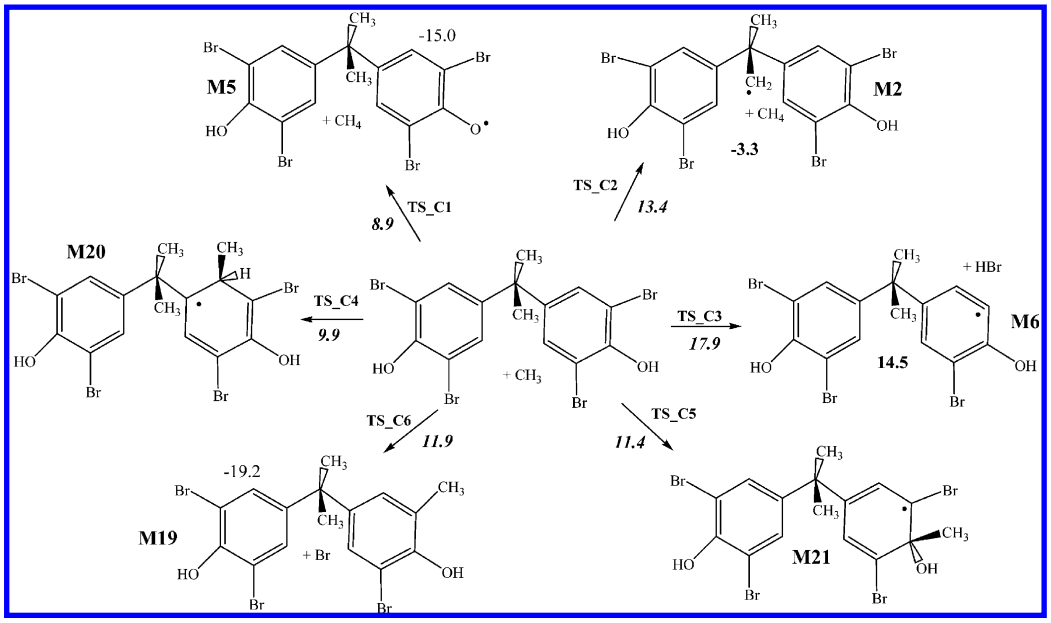

Figure 9. PES for the decomposition of TBBA in bimolecular reactions with a methyl group. Values in bold and italics signify reaction and activation energies at 0.0 K.

Scheme 2

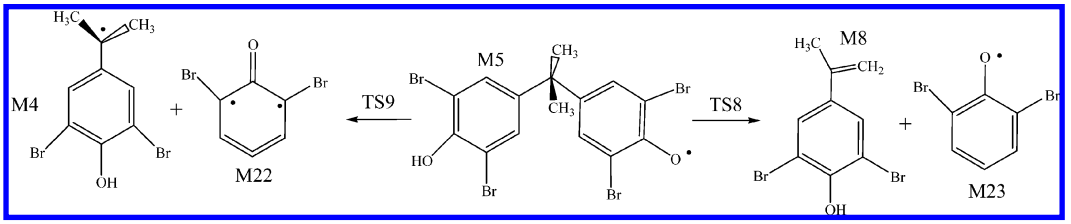

62.0 kcal/mol). As evident from the calculated reaction rate constants in Table 1, direct scission of the C−C linkage through TS9 outpaces the intramolecular hydrogen migration by several orders of magnitude, at all considered temperatures.

4. CONCLUSIONS

We have developed a new mechanism for the initiation reaction of the pyrolysis of tetrabromobisphenol A (TBBA). We have derived thermochemical as well as mechanistic and kinetic parameters related to the self-decomposition of TBBA and its bimolecular reactions with H, Br, and CH_3 radicals. A loss of a methyl group, followed by the β C−H bond cleavage, marks the most preferred pathway in the unimolecular decomposition of TBBA. The previously proposed fission of the isopropylidene linkage appears to be of negligible importance at all temperatures. Abstraction of hydroxyl H atoms constitutes the most important channel in the bimolecular reactions of TBBA with Br and CH_3 radicals. Reactions of H and Br with TBBA provide an important source for the formation of HBr, a major product observed in experimental studies.

■ ASSOCIATED CONTENT

Supporting Information

Figure S1, Cartesian coordinates, total energies, and vibrational frequencies for all structures. This material is available free of charge via the Internet at http://pubs.acs.org.

■ AUTHOR INFORMATION

Corresponding Author

*E-mail: M.Altarawneh@Murdoch.edu.au. Phone: (+61) 8 9360-7507.

Present Address

†M.A.: On leave from Chemical Engineering Department, Al-Hussein Bin Talal University, Ma'an, Jordan.

Notes

The authors declare no competing financial interest.

■ ACKNOWLEDGMENTS

This study has been supported by a grant of computing time from the National Computational Infrastructure (NCI), Australia as well as funds from the Australian Research Council (ARC). We thank an anonymous reviewer for his/her detailed comments.

■ REFERENCES

(1) Alaee, M.; Arias, P.; Sjödin, A.; Bergman, Å. An Overview of Commercially Used Brominated Flame Retardants, Their Applications, Their Use Patterns in Different Countries/Regions and Possible Modes of Release. *Environ. Int.* **2003**, *29*, 683−716.

(2) Quan, C.; Li, A.; Gao, N. Research on Pyrolysis of PCB Waste with TG-FTIR and Py-GC/MS. *J. Therm. Anal. Calorim.* **2012**, *110*, 1463−1470.

(3) Alaee, M. Recent Progress in Understanding of the Levels, Trends, Fate and Effects of BFRs in the Environment. *Chemosphere* **2006**, *64*, 179−180.

(4) Bart, J. C. J. Polymer/Additive Analysis by Flash Pyrolysis Techniques. *J. Anal. Appl. Pyrol* **2001**, *58*−*59*, 3−28.
(5) Bozi, J.; Czégény, Z.; Mészáros, E.; Blazsó, M. Thermal Decomposition of Flame Retarded Polycarbonates. *J. Anal. Appl. Pyrol* **2007**, *79*, 337−345.
(6) Font, R.; Moltó, J.; Ortuño, N. Kinetics of Tetrabromobisphenol A Pyrolysis. Comparison between Borrelation and Mechanistic Models. *J. Anal. Appl. Pyrol* **2012**, *94*, 53−62.
(7) Grause, G.; Furusawa, M.; Okuwaki, A.; Yoshioka, T. Pyrolysis of Tetrabromobisphenol-A Containing Paper Laminated Printed Circuit Boards. *Chemosphere* **2008**, *71*, 872−878.
(8) Luda, M. P.; Balabanovich, A. I.; Zanetti, M. Pyrolysis of Fire Retardant Anhydride-Cured Epoxy Resins. *J. Anal. Appl. Pyrol* **2010**, *88*, 39−52.
(9) Marongiu, A.; Bozzano, G.; Dente, M.; Ranzi, E.; Faravelli, T. Detailed Kinetic Modeling of Pyrolysis of Tetrabromobisphenol A. *J. Anal. Appl. Pyrol* **2007**, *80*, 325−345.
(10) Sonnier, R.; Otazaghine, B.; Ferry, L.; Lopez-Cuesta, J.-M. Study of the Combustion Efficiency of Polymers Using A Pyrolysis−Combustion Flow Calorimeter. *Combuts. Flame* **2013**, *160*, 2182−2193.
(11) Thies, J.; Neupert, M.; Pump, W. Tetrabromobisphenol A (TBBA), Its Derivatives and Their Flame Retarded (FR) Polymers — Content of Polybrominated Dibenzo-p-dioxins (PBDD) and Dibenzofurans (PBDF) — PBDD/F Formation under Processing and Smouldering (Worst Case) Conditions. *Chemosphere* **1990**, *20*, 1921−1928.
(12) Luda, M. P.; Balabanovich, A. I.; Hornung, A.; Camino, G. Thermal Degradation of a Brominated Bisphenol A Derivative. *Polymer. Adv. Technol.* **2003**, *14*, 741−748.
(13) Lorenz, W.; Bahadir, M. Recycling of Flame Retardants Containing Printed Circuits: A Study of the Possible Formation of Polyhalogenated Dibenzodioxins/-Furans. *Chemosphere* **1993**, *26*, 2221−2229.
(14) Yang, X.; Sun, L.; Xiang, J.; Hu, S.; Su, S. Pyrolysis and Dehalogenation of Plastics from Waste Electrical and Electronic Equipment (WEEE): A Review. *Waste Manage.* **2013**, *33*, 462−473.
(15) Barontini, F.; Cozzani, V.; Marsanich, K.; Raffa, V.; Petarca, L. An Experimental Investigation of Tetrabromobisphenol A Decomposition Pathways. *J. Anal. Appl. Pyrol* **2004**, *72*, 41−53.
(16) Marsanich, K.; Zanelli, S.; Barontini, F.; Cozzani, V. Evaporation and Thermal Degradation of Tetrabromobisphenol A above the Melting Point. *Thermochim. Acta* **2004**, *421*, 95−103.
(17) Altarawneh, M.; Dlugogorski, B. Z. A Mechanistic and Kinetic Study on the Formation of PBDD/Fs from PBDEs. *Environ. Sci. Technol.* **2013**, *47*, 5118−5127.
(18) Frisch, M. J.; Trucks, G. W.; Schlegel, H. B.; Scuseria, G. E.; Robb, M. A.; Cheeseman, J. R.; Scalmani, G.; Barone, V.; Mennucci, B.; Petersson, G. A.; et al. *Gaussian 09*, revision A.1; Gaussian, Inc: Wallingford, CT, 2009.
(19) Zhao, Y.; Truhlar, D. The M06 Suite of Density Functionals for Main Group Thermochemistry, Thermochemical Kinetics, Noncovalent Interactions, Excited States, and Transition Elements: Two New Functionals And Systematic Testing of Four M06-Class Functionals and 12 Other Functionals. *Theor. Chem. Acc.* **2008**, *120*, 215−241.
(20) Montgomery, J. J. A.; Ochterski, J. W.; Petersson, G. A. A Complete Basis Set Model Chemistry. IV. An Improved Atomic Pair Natural Orbital Method. *J. Chem. Phys.* **1994**, *101*, 5900−5909.
(21) Wigner, E. On the Quantum Correction for Thermodynamic Equilibrium. *Phys. Rev.* **1932**, *40*, 749−759.
(22) Wardlaw, D. M.; Marcus, R. A. RRKM Reaction Rate Theory for Transition States of Any Looseness. *Chem. Phys. Lett.* **1984**, *110*, 230−240.
(23) Mokrushin, V. B. V.; Tsang, W.; Zachariah, M.; Knyazev, V. *ChemRate*. V.1.19 ed.; NIST: Gaithersburg, MD, 2002.
(24) Eriksson, J.; Eriksson, L. 2,2′,6,6′-Tetrachloro-4,4′-propane-2,2-diyldiphenol, 2,2′,6-Tribromo-4,4′-propane-2,2-diyldiphenol and 2,2′,6,6′-Tetrabromo-4,4′-propane-2,2-diyldiphenol. *Acta Crystallogr., Sect. C* **2001**, *57*, 1308−1312.
(25) Qiu, S.; Wei, J.; Pan, F.; Liu, J.; Zhang, A. Vibrational, NMR Spectrum and Orbital Analysis of 3,3′,5,5′-Tetrabromobisphenol A: A Combined Experimental and Computational Study. *Spectrochim. Acta, Part A* **2013**, *105*, 38−44.
(26) Afeefy, H. Y.; Liebman, J. F.; Stein, S. E.; Linstrom, P. J.; Mallard, W. G. *NIST Chemistry WebBook, NIST Standard Reference Database Number 69*; NIST: Gaithersburg, MD, 2005.
(27) Luo, R. Y. *Handbook of Bond Dissociation Energies in Organic*; CRC Press: Boca Raton, FL, 1999.
(28) Altarawneh, M.; Dlugogorski, B. Z.; Kennedy, E. M.; Mackie, J. C. Quantum Chemical and Kinetic Study of Formation of 2-Chlorophenoxy Radical from 2-Chlorophenol: Unimolecular Decomposition and Bimolecular Reactions with H, OH, Cl, and O_2. *J. Phys. Chem. A* **2008**, *112*, 3680−3692.
(29) Truhlar, D. G.; Garrett, B. C. Variational Transition State Theory. *Annu. Rev. Phys. Chem.* **1984**, *35*, 159−189.
(30) Bearpark, M. J.; Ogliaro, F.; Vreven, T.; Boggio-Pasqua, M.; Frisch, M. J.; Larkin, S. M.; Morrison, M.; Robb, M. A. CASSCF Calculations for Photoinduced Processes in Large Molecules: Choosing When to Use the RASSCF, ONIOM and MMVB approximations. *J. Photochem. Photobiol., A* **2007**, *190*, 207−227.
(31) Kitagawa, Y.; Saito, T.; Ito, M.; Shoji, M.; Koizumi, K.; Yamanaka, S.; Kawakami, T.; Okumura, M.; Yamaguchi, K. Approximately Spin-Projected Geometry Optimization Method and Its Application to Di-chromium Systems. *Chem. Phys. Lett.* **2007**, *442*, 445−450.
(32) Takahara, Y.; Yamaguchi, K.; Fueno, T. Potential Energy Curves of Fluorine, Nitrogen and Ethylene Calculated by Approximately Projected Unrestricted Hartree−Fock and Møller−Plesset Perturbation Methods. *Chem. Phys. Lett.* **1989**, *157*, 211−216.
(33) Robaugh, D. A.; Stein, S. E. Stabilities of Highly Conjugated Radicals from Bond Homolysis Rates. *J. Am. Chem. Soc.* **1986**, *108*, 3224−3229.
(34) Sivaramakrishnan, R.; Michael, J. V.; Harding, L. B.; Klippenstein, S. J. Shock Tube Explorations of Roaming Radical Mechanisms: The Decompositions of Isobutane and Neopentane. *J. Phys. Chem. A* **2012**, *116*, 5981−5989.
(35) Altarawneh, M.; Dlugogorski, B. Z.; Kennedy, E. M.; Mackie, J. C. Mechanisms For Formation, Chlorination, Dechlorination and Destruction of Polychlorinated Dibenzo-*p*-Dioxins And Dibenzofurans (PCDD/Fs). *Prog. Energy Combust. Sci.* **2009**, *35*, 245−274.
(36) Alecu, I. M.; Gao, Y.; Hsieh, P. C.; Sand, J. P.; Ors, A.; McLeod, A.; Marshall, P. Studies of the Kinetics and Thermochemistry of the Forward and Reverse Reaction Cl + C_6H_6 = HCl + C_6H_5. *J. Phys. Chem. A* **2007**, *111*, 3970−3976.
(37) Liu, R.; Morokuma, K.; Mebel, A. M.; Lin, M. C. Ab Initio Study of the Mechanism for The Thermal Decomposition of the Phenoxy Radical. *J. Phys. Chem.* **1996**, *100*, 9314−9322.